MicroRNA Profiles Associated with Bone Healing of the Extraction Socket in Medication-Related Osteonecrosis of the Jaw in Rat Model: A Pilot Study

Thapakorn Surajkulwatana[1*], Anjalee Vacharaksa[2], and Supreda Suphanantachat Srithanyarat[3, 4]

[1]Master of Science Program in Geriatric Dentistry and Special Patients Care (International Program), Faculty of Dentistry, Chulalongkorn University, Bangkok, Thailand
[2]Department of Microbiology, Faculty of Dentistry, Chulalongkorn University, Bangkok, Thailand
[3]Department of Periodontology, Faculty of Dentistry, Chulalongkorn University, Bangkok, Thailand
[4]Genomics and Precision Dentistry Research Unit, Faculty of Dentistry, Chulalongkorn University, Bangkok, Thailand
[*]Corresponding author, E-mail: 6075843832@student.chula.ac.th

Abstract

Bisphoshonates (BPs) are widely used for treating osteoporosis, multiple myeloma, breast cancer, and bone metastasis cancer. Trauma or tooth extraction in patients treated with BPs can lead to MRONJ development because of its mechanism of action by which interferes bone homeostasis and angiogenesis. Once MRONJ has occurred, this hard-to-cure disease posed the risk of having poor quality of life to the patients. The application of miRNA for curing the diseases is now being of interest in the medical field. Aiming at elucidating the role of miRNAs in the pathogenesis of MRONJ, a rat model was used in creating MRONJ and the expression of candidate miRNAs was evaluated in this study. Twelve rats were randomly divided into 3 groups; 1) zolendronate plus dexamethasone-treated group (Zol), 2) dexamethasone-treated group as a vehicle (Dex), and 3) control group which receiving normal saline solution (NSS). Tooth extraction was performed after 2 weeks of BPs administration. The MRONJ occurred in extraction sockets were confirmed by clinical appearances which are micro-CT, and histological analysis at Day14 and 28 post-extraction. Bone samples from extraction sites were collected for miRNA analysis. In this study, MRONJ in a rat model was successfully established in Zol group. The miRNA analysis revealed an upregulation of 6 candidate miRNAs involving in an inhibition of osteoblast maturation (miR-23a-3p, miR-23b-3p, miR27a-3p and miR-24-3p) and anti-angiogenic activity (miR-34-5p and miR-652-3p). The expression of miR-23a-3p and miR-23b-3p were 12- to 14-fold upregulation comparing with the control group. This study suggested the certain miRNAs, especially miR-23, affected the development of MRONJ.

Keywords: *Angiogenesis, Medication-related osteonecrosis of the jaw, Bone remodeling, Micro-computed tomography, MicroRNA*

1. Introduction

Medication-related osteonecrosis of the jaw (MRONJ) could be found in patients who take antiresorptive or antiangiogenic drugs especially bisphosphonates (BPs) for the treatment of cancer and osteoporosis. Tooth extraction or trauma to jaw bone can lead to MRONJ in these patients. Patients are distressed from MRONJ symptoms as having pain, swelling, cellulites, halitosis, and trismus. Intraoral examination finds bone exposure at upper or lower jaw, a pathologic fracture, an oral-cutaneous fistula, or a presence of infection that cause physical pain, and psychological problems that effect to speaking, swallowing and eating ability resulted in worsen quality of life (Miksad et al, 2011; S. L. Ruggiero et al, 2014).

The incidence of MRONJ varies among many studies depending on a type of disease. The incidence of MRONJ in cancer patients is higher than MRONJ in osteoporosis patients. The range varies from 0.8 to 12% (Kühl, Walter, Acham, Pfeffer & Lambrecht, 2012). Zoledronic acid (ZA) (5 mg/year) injection is used for treating patients with menopausal osteoporosis (Black et al, 2007). ZA is also recommended for treatment of malignant tumor and multiple myeloma. Recommended dose is 4 mg as a single-use intravenous infusion over no less than 15 minutes every 3-4 weeks.

The use of BPs aims to abrogate metastasis of cancer via anti-angiogenesis effect and impede bone resorption activity in osteoporosis which affects through both osteoclastic and osteoblastic activity (S. L. Ruggiero et al, 2014). BPs could have anti-angiogenic activity which in turn restricted the pathway of nutrient and oxygen transportation, immunized cells infiltration and also reduced serum VEGF levels

(Nissen et al, 1998). BPs could also inhibit osteoclastic activity, which led to a reduction in the activation of osteoblasts. Consequently, bone formation was arrested due to a decrease of osteoblastic activity (Ganda, 2013). These effects of BPs appeared to severely impact the wound healing of jaw bone.

The dental treatment strategy of MRONJ depends on the stage of disease. Patients who have risk of MRONJ should be monitored signs and symptoms that may occur during a treatment. The benefit of an early treatment by prescribing analgesic drugs, antibiotics, or 0.12% chlorhexidine mouthwash to the patients who have pain or discomfort in upper or lower jaw for pain and infection control. Patients who have a sequestrum and exposed bone were benefited from debridement. In some severe cases, a need to resect an infected bone may offer long-term palliation with a resolution of acute infection and pain. Symptomatic patients with late stage may require resection and immediate rehabilitation with a reconstruction plate or an obturator (S. L. Ruggiero et al, 2014). This in turn posed a poor quality of life to the patient who suffering from MRONJ.

Currently, microRNAs (miRNAs) associated with many diseases have been found in the human genome. MiRNA can regulate or find-tune the expression of DNA, resulting in protein formation or suppression of protein production (Bartel, 2004; Fish et al, 2008; Harris, Yamakuchi, Ferlito, Mendell & Lowenstein, 2008; Wu, Yang & Li, 2009). The application of miRNA for curing the diseases is the forefront field in medicine presently. To our knowledge, the studies related to the target miRNAs that play a role in controlling the effect of BPs in the healing of the jaw bone is still lacking. In searching of the target miRNAs involved in the pathogenesis of MRONJ, this study aims to investigate the candidate miRNAs associated with MRONJ in a rat model. The future application of target miRNAs may provide a promising alternative administration for the treatment of MRONJ.

2. Objectives

To investigate miRNA profiles associated with bone healing in a rat model of medication-related osteonecrosis of the jaw.

3. Materials and Methods

The animal model

The animal protocol was approved by Chulalongkorn University Animal Care and Use Committee (protocol number 1873005). Twelve Sprague Dawley (SD) rats (6-week-old), weight range (195-205 g) were quarantined in a laboratory environment for 2 weeks and randomly divided into 3 groups;

Group 1; Zol (n = 6): administration of zoledronate (66 µg/kg; Zometa, Novartis Pharma, Stein AG, Stein, Switzerland) and dexamethasone (5 mg/kg; Dexton, T.P. Drug Laboratory, Bangkok, Thailand).

Group 2; Dex (n = 3): administration of dexamethasone (5 mg/kg) as a vehicle group

Group 3; NSS (n = 3): administration of normal saline solution (Klean&Kare, Bangkok, Thailand) as a control group

Each experimental group were injected intraperitoneally with either zoledronate, dexamethasone, or normal saline solution every 2-3 days for 4 weeks. Two weeks after the first drug administration (Day 0), the maxillary first molar was extracted under general anesthesia. Experimental design, interventions and timeline of experiment are shown in Figure 1.

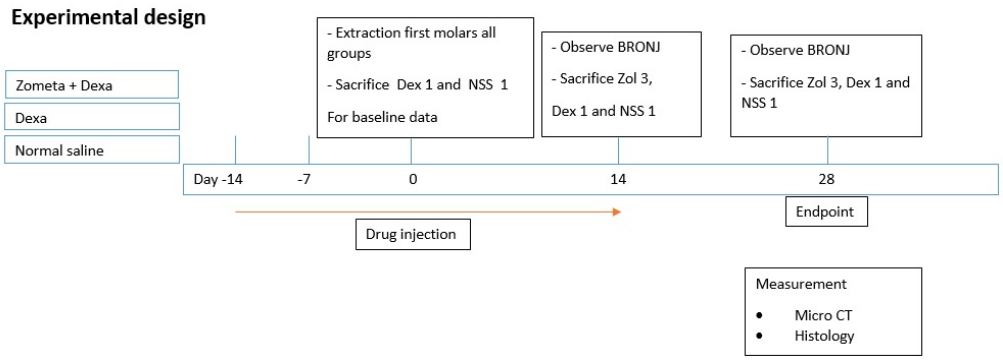

Figure 1 Experimental design and timeline

- Tooth extraction

General anesthesia was performed by intraperitoneal injection of tiletamine-zolazepam (Zoletil; 40 mg/kg) and xylazine (2 mg/kg), providing a duration of 30 minutes under anesthesia. Then, the maxillary first molars from both sides were extracted with an explorer no.5 and artery forceps.

- Post-operative care

Rats were monitored until being fully recovered from general anesthesia. Opioid analgesic drug was prescribed subcutaneously for 3 days. The soft diet was ordered for all rats after tooth extraction for 7 days and was changed to normal diet after Day 7 post-extraction. During the experiment, the rats were observed and weighed every 2 days to ensure the normal eating behavior and adequate nutrition.

- Euthanasia and harvesting of sample specimens

Animals were sacrificed on Day 0, 14, and 28 after extraction by inhalation of CO_2 and cardiac puncture. Confirmation of death was done before harvesting the maxilla. An occurrence of MRONJ in Zol group was confirmed by visual inspection on the epithelial closure and bone exposure after 4 weeks of tooth extraction (Zandi et al, 2016). The photographs of the maxilla were taken in each group. Then, the maxillary tissues were dissected and removed. The samples of the maxilla were separated into halves antero-posteriorly. The first half was used as the bone sample for microRNA analysis. Another half of the maxilla was fixed in 10% formalin for further micro-CT and histological analysis.

Micro – CTs analysis

The characteristic of bone formation in the extraction sockets at Day 14 and 28 after extraction was visualized using a micro-computed tomography (CT) system (SCANCO Medical, Brüttisellen, Switzerland) at the Mineralized Tissue Research Unit, Faculty of Dentistry, Chulalongkorn University. The maxillary bones were scanned using micro-CT with an X-ray source of 70 kV/113µA with a slice thickness of 15 µm.

Proceedings of RSU International Research Conference (2020)

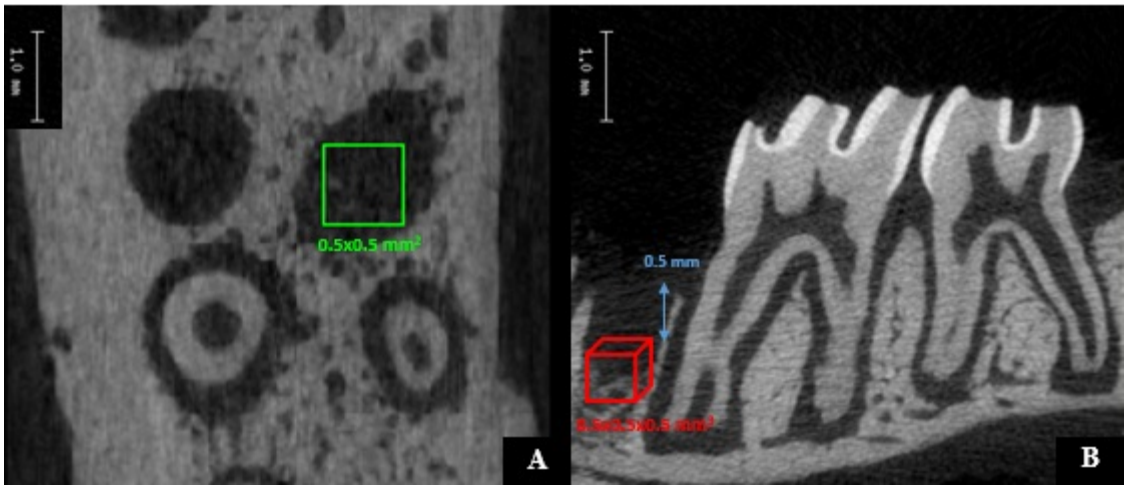

Figure 2 Setting of the region of interest (ROI) and volume of interest (VOI) in an extraction socket.

To assess new bone formation, a region of interest (ROI) was established in a micro-CT image. The axial view was used to identify the interproximal crestal bone between the upper second molar and the extraction socket. The micro-CT slice which represented the distance of 0.5 mm apical to the first identifiable alveolar crest was selected as the slice of interest. Then, the ROI was created by making the square with the size of 0.5 x 0.5 mm^2 at the center of an extraction socket on this slice (Figure 2A). In order to determine bone volume in the extraction socket, the volume of interest (VOI) of 0.5 x 0.5 x 0.5 mm^3 per extraction socket was established by using the ROI as a reference (Figure 2B). Bone volumes and gross 3D images were processed and compared among groups using ImageJ software (Fiji, NIH, USA) and 3D viewer (Microsoft, USA).

Histological analysis

After being fixed in 10% formalin, the tissue samples were decalcified with 0.1mol/l EDTA and embedded in paraffin. The anterior border of tissue was at the last rugae presented distal to an upper incisor and the posterior border was 0.5 mm distal to the third molar. Samples were trimmed and cut in sagittal section in 5-mm thickness using a microtome. These fixed tissues were stained with the hematoxylin and eosin (H&E) solution. At the extraction site, a presence of osteocyte in lacuna was determined, and the number of empty lacunae was counted by using Photoshop CC (Adobe systems Incoporated, California, U.S.A).

MiRNA analysis

The bone sample was collected from an extraction socket with a 2 mm-diameter trephine bur and then kept in RNAlater (Qiagen, Valencia, CA, USA). The bone tissue was homogenized by metal beads (size 2.38 mm; Qiagen, Valencia, CA, USA) with a homogenizer machine (Powerlyzer™ 24; Qiagen, Valencia, CA, USA). Total miRNAs were extracted by miReasy mini kit (Qiagen, Valencia, CA, USA) and quantified yield concentration using the Nano-Drop® ND-1000 ultraviolet spectrophotometer (Thermo Scientific, Wilmington, DE, USA). Total RNA samples were converted to cDNA using miScript II RT Kit (Qiagen, Hilden, Germany) on thermal cycler, and the real-time PCR was performed using Quantitect SYBR Green PCR mastermix (Qiagen, Hilden, Germany) following the manufacturer's instructions. The candidate microRNAs investigated in this study are shown in Table 1. Customized primers were designed and supplied by GeneGlobe (Qiagen, Valencia, CA, USA) in customized 96-well plate qPCR array. The list of primers is shown in Table 2. After collected data from CFX Connect Real-Time PCR Detection System (Bio-Rad, Hercules, CA, USA), raw quantification cycle values (Ct) were collected. The Ct values > 35 were considered to be excluded. Whereas, only the miRNAs with a Ct ≤ 35 were used in experiment, then Ct was normalized by constitutive genes (miR-16-5p and miR-423-3p) using $2^{-\Delta\Delta ct}$ method.

Statistical analysis

An incidence of MRONJ, bone volume in healing sockets, number of empty osteocytes, and fold changes of miRNA expression were reported and analyzed in a descriptive manner due to the limited number of study sample.

Table1 List of candidate miRNAs in MRONJ rat model

Mechanism	miRNAs	Target gene	Reference
Anti - angiogenic activity	miR-34a-5p	SIRT1	Lian et al, 2012
	miR-652-3p	Cyclin D2	Huang et al, 2019
	miR-663	TGF-β1	Hong et al, 2015
			Michaille et al, 2018
	miR-720	VASH1	Wang et al, 2014
Promote - osteoblastic activity	miR-34a	Cyclin D1, NOTCH1	Fan et al, 2016
Inhibit - osteoblastic activity	miR-23a-3p	RUNX2	Hassan et al, 2010
	miR-23b-3p	RUNX2	Guo et al, 2016
	miR-27a-3p	HOXA10, RUNX2	Lian et al, 2012
	miR-24-3p	RUNX2, Tcf-1	Zhao et al, 2015

Table2 Designed primer of candidate miRNAs

miRBase Accession No.	Mature miRNA ID	miScript Primer Assay Catalog
MIMAT0000255	hsa-miR-34a-5p	MS00003318
MIMAT0003322	hsa-miR-652-3p	MS00010451
MIMAT0003326	hsa-miR-663a	MS00037247
MIMAT0005954	hsa-miR-720	MS00014833
MIMAT0000078	hsa-miR-23a-3p	MS00031633
MIMAT0000418	hsa-miR-23b-3p	MS00031647
MIMAT0000084	hsa-miR-27a-3p	MS00003241
MIMAT0000080	hsa-miR-24-3p	MS00006552

4. Results and Discussion

Results

Animal model

From total animal samples (N = 12), there was 3 rats died during the course of experiment. In Zol group, one rat died during the blood collection procedure due to the heart attack. Another 2 rats from NSS and Dex group died immediately after tooth extraction due to overdosage of anesthetic drug and nephrotoxicity. Therefore, at Day 14 after extraction, there were 7 rats remaining in this study, resulting in an inadequate number of study samples in NSS and Dex group at the endpoint of analysis. Accordingly, only the descriptive analysis of the results could be performed.

Gross evaluation

Four weeks after tooth extraction, the extraction sockets in both NSS and Dex groups showed normal wound healing (Figure 3A&B). In contrast, brownish color sockets and bone exposure in which indicated the MRONJ appearance were observed in all rats belonged to Zol group (Figure 3C). The percentage of bone exposure in each group is shown in Figure 4.

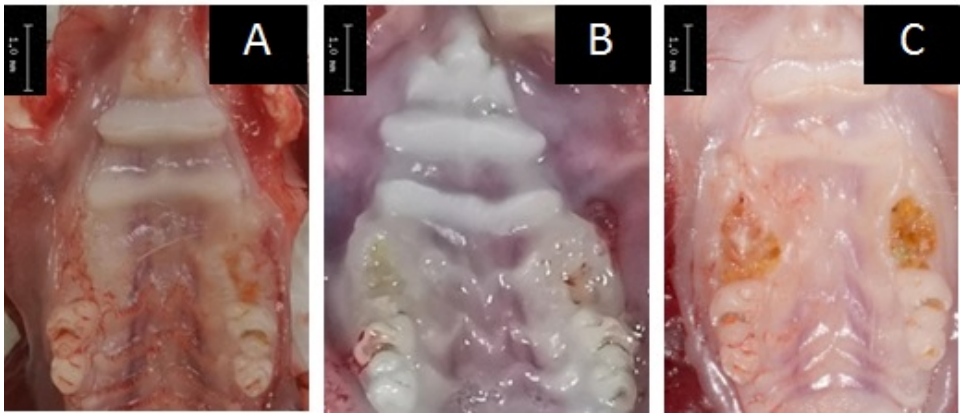

Figure 3 Gross evaluation: 28 days after extraction, (A) normal saline administration (NSS), (B) dexamethasone administration (Dex), (C) zoledronate and dexamethasone administration (Zol)

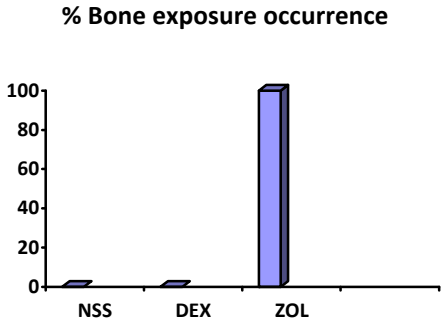

Figure 4 % Bone exposure occurrence (N=5)

Micro-CT analysis

Micro-CT analysis revealed delayed bone formation and irregular trabeculae bone arrangement in the extraction sockets of the Zol group while normal bone formation and trabeculae bone forming were observed in NSS and Dex groups. The rendering 3D characteristic of bone formation comparing among NSS, Dex and Zol group at Day 28 was performed and demonstrated in Figure 5. The lowest amount of calcification was seen in Zol group. Calcification volume was quantified at Day 14 and 28 after tooth extraction. Bone volume of newly formed bone in VOI were 0.0943 mm^3 (SE 0.0074 mm^3) in NSS group and 0.0912 mm^3 in Dex group. In the group of rats that were treated with zolendronate, after 14 and 28 days of extraction (Zol-14 and Zol-28) the bone volume of 0.0340 mm^3 (SE 0.0176 mm^3) and 0.0195 mm^3 (SE 0.0076 mm^3) was observed, respectively (Figure 6).

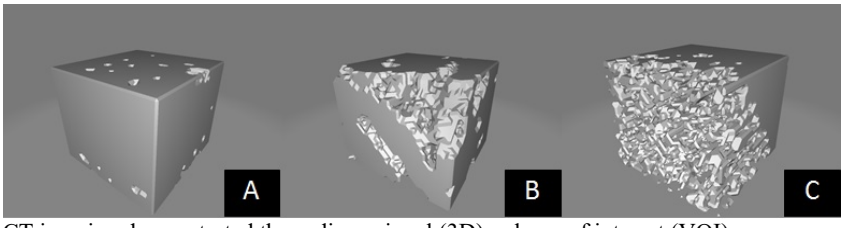

Figure 5 Micro-CT imaging demonstrated three-dimensional (3D) volume of interest (VOI).
(A) normal saline administration (NSS), (B) dexamethasone administration (Dex),
(C) zoledronate plus dexamethasone administration (Zol)

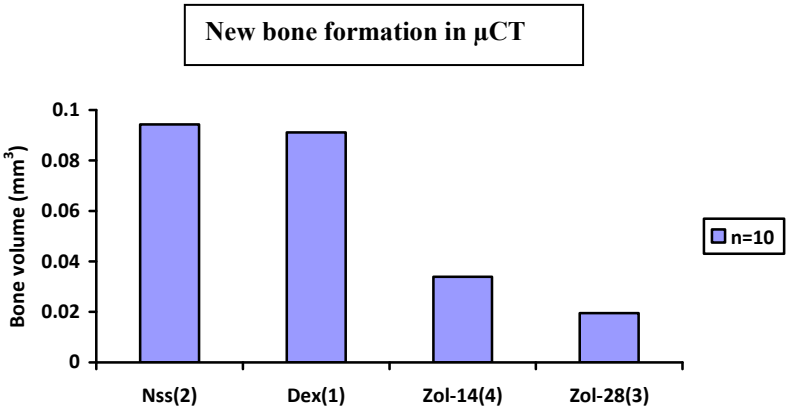

Figure 6 New bone formation (mm^3) at Day 28 after extraction analyzed by µCT in each group (data calculated per socket; n=10)

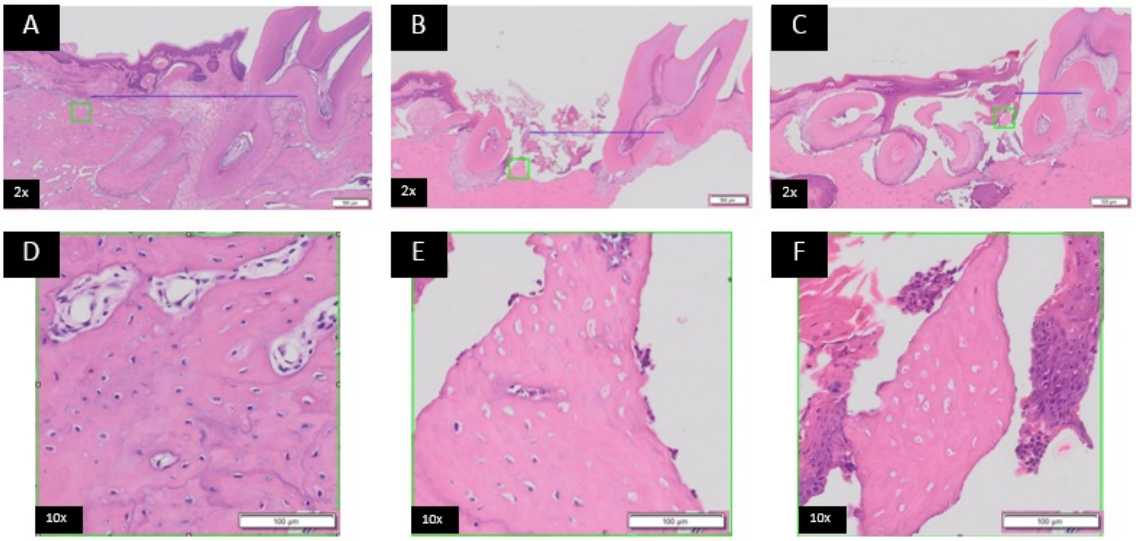

Figure 7 Histological images revealed complete epithelial coverage and bone healing was found in the control group 28 days (A). A lack of mucosal lining in the extraction socket and abnormal bone remodeling could be observed in Zol group after 14 days and 28 days of extraction (B, C); scale bar: 500 µm. Enlarged images of the square areas in 10X (D-F); scale bar: 100 µm.

Histological analysis

Histological images showed complete epithelial coverage and normal wound healing in the control group (Figure 7A). Whereas, a lack of epithelial lining and poor bone formation were observed in the extraction socket of BP-treated group (Figure 7B&C). There was also detectable bacterial colonization and found abundant inflammatory cells in extraction sites of the BP-treated animals two weeks after extraction (Figure 7B). Histopathological images also demonstrated the higher number of empty osteocyte lacunae in both BP-treated group compared to the control group (Figure 7 D-F). The highest percentage of empty osteocyte in lacunae was observed in Zol-28 group followed by Zol-14 and NSS group (59.05%, 33.77%, and 12.6%, respectively).

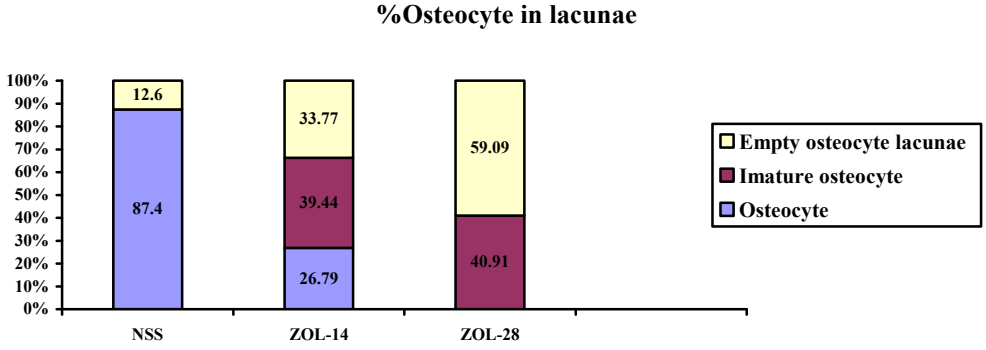

Figure 8 Percentage of osteocyte in lacunae determined at Day 14 and Day 28 after extraction.

MiRNA analysis

For miRNA analysis, the miRNA expression level in bone tissue samples obtained from Zol-treated group and NSS-group at Day 28 after tooth extraction were compared. From total 8 candidate miRNAs, 6 miRNAs showed the expression in customized miRNA PCRarray (Figure 9). miR-23a-3p and miR-23b-3p, that involved in inhibition of osteoblastic activity, were 12- to 14-fold upregulated in zoledronate plus dexamethasone treated group. A moderate expression was found in miR-34a-5p and miR-24-3p (5- and 4.5-fold upregulation, respectively). Moreover, miR-27a-3p and miR-652-3p were upregulated approximately 3 and 1.5 folds higher than a normal saline treated group. In contrast, there were no difference in the expression of miR-663a and miR720 between 2 groups.

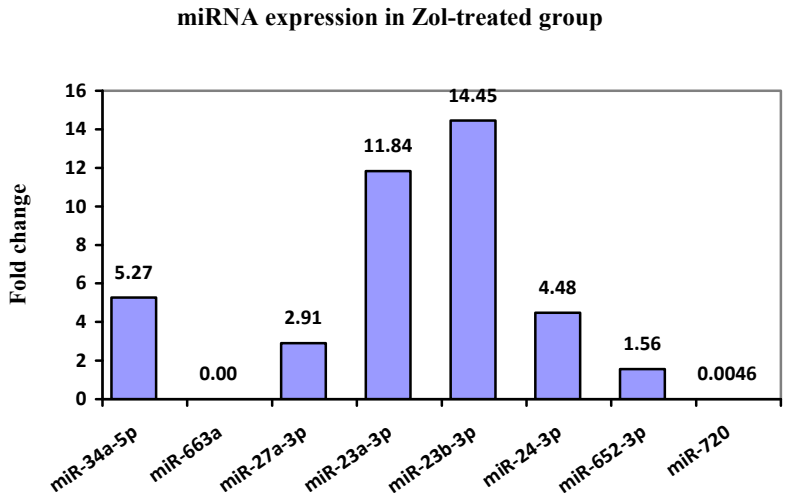

Figure 9 The normalized expressions of target miRNAs (fold change) in comparison between Zol-treated group and control group (NSS-group) at Day 28 post-extraction.

Discussion

Medication-related osteonecrosis of the jaw (MRONJ) has been recognized for decades. However, the underlying pathophysiologic mechanisms of MRONJ in both cellular and molecular level is still unclear. Although several treatment options for MRONJ patients have been introduced, those treatments are able to help patients only at a palliative care level. In current study, the MRONJ was created by an

administration of zoledronate plus dexamethasone in SD rat models. The expressions of miRNAs targeted at angiogenic, osteoblastic, and osteoclastic activity in MRONJ-bone tissue samples were investigated.

According to the definition of MRONJ in human is exposed bone, having fistula, incomplete wound healing and epithelial lining for more than 8 weeks (Ruggiero, Dodson & Fantasia, 2014). In this present study, the established MRONJ lesion in rat models could be observed by gross visualization showing incomplete mucosal coverage and necrotic bone at 2 and 4 weeks after extraction. This similar time point of MRONJ occurrence has been reported in previous studies of rat models treated with zoledronate injection (Howie et al, 2015; Kaibuchi, Iwata, Yamato, Okano & Ando, 2016; Kuroshima et al, 2018). A micro-CT analysis of hard tissue characteristics revealed the poorly formed bony structure in the extraction socket of rats receiving zoledronate-dexamethasone injection as shown in the 3D rendering images compared to the control groups. To quantify the healing capacity of alveolar bone, the bone volume in extraction sockets at day 14 and 28 after extraction were calculated. The bone volume of Zol group observed at day 14 and 28 were smaller than those of the control groups. Five-fold smaller bone volume could be observed in Zol-28 group compared to NSS-28 group. Kuroshima et al. also reported the 50% lesser bone fill in extraction sockets after being injected with zoledronate/cyclophosphamide than those of a control group at 7 weeks after extraction (Kuroshima et al, 2018). Another similar study also demonstrated a percentage of calcification volume in extraction sockets of zoledronate/dexamethasone-treat group with a twice lower percentage than the untreated group (Kaibuchi et al, 2016). The differences in results may be due to different types of the rat used, drug administration, and calculation methods. Interestingly, within Zol groups, a bone volume of healing sockets after tooth extraction for 28 days was twice smaller than those of the 14-day extraction sockets. This result assured the methods in establishing MRONJ lesion and also suggested that the MRONJ occurrence could be early notified at 2 weeks after tooth extraction in rat model.

In histological study, H&E staining demonstrated normal wound healing with intact epithelium and connective tissue in the extraction socket of NSS group while in both 14- and 28-day zoledronate treated groups showed incomplete wound healing, detached epithelium and dense inflammatory cells infiltration. The healing of alveolar sockets in NSS group demonstrated new bone formation with 87.4% healthy osteocytes in lacunae. In contrast, a number of empty osteocyte lacunae was remarkably lower in Zol-28 group which showed 59.1% empty lacunae. This result corresponded with the previous study that approximately 3-fold higher number of empty osteocyte lacunae could be observed comparing with that of the control NSS group (Kuroshima et al, 2018). Furthermore, with high magnification, a higher number of osteoclasts could be observed microscopically in Zol-28 group than those of the Zol-14 and NSS group.

To understand a molecular mechanism controlling the pathogenesis of MRONJ, the roles of miRNAs in MRONJ development have been studied. As the key mechanisms that propagate MRONJ are an inhibition of angiogenesis and a promotion of osteoclastic activity, 8 candidate miRNAs that previously reported as having important roles in angiogenic activity and bone remodeling were chosen and evaluated. In this study, miRNAs targeting at RUNX2 (Runt-related transcription factor 2) suppression including miR-23a-3p, miR-23b-3p, miR27a-3p and miR-24-3p were found to be upregulated. Previous studies have demonstrated the miR-23a~27a~24-2 cluster was one of 11 miRNAs that has been identified as negative tuning on RUNX2, which in turn suppressing osteoblast differentiation (Zhang et al, 2011) (Lian et al, 2012). An inhibitory role of the miR-23a on RUNX2 and special AT-rich sequence-binding protein-2 (SATB2) in mesenchymal cells which resulting in suppression of osteoblast maturation has also been reported (Zhang et al, 2011). In MRONJ rat models, miR23a was noted as one of the candidates circulating biomarkers to diagnose MRONJ (Yang, Tao, Wang, Shuai & Jin, 2018). Likewise, miR-27a has been reported as having a role in regulating RUNX2 via HOXA10 inhibition and resulted in inhibiting osteoblastogenesis (Lian et al, 2012). The results from this study indicated the role of miR-23a-3p, miR-23b-3p, miR27a-3p and miR-24-3p in impeding an osteoblastic maturation in MRONJ and miR-23, via RUNX2, might play an important role in propagating MRONJ lesion.

In our study, a 5-fold upregulation of miR-34a-5p expression was observed in MRONJ extraction sockets. According to the researches, miR-34a involved in both bone remodeling and angiogenic activity. In irradiated bone defects, miR-34a could promote bone regeneration by inducing an osteoblastic

Proceedings of RSU International Research Conference (2020)

differentiation of bone marrow stromal cells (BSMCs) via NOTCH1 targeting (Liu et al, 2019). In angiogenesis, miR-34a-5p decreased the number of vessels by inhibiting a function of the silent information regulator 1 (SIRT1)(Ito, Yagi & Yamakuchi, 2010). Regarding an anti-angiogenic activity, however, there was no difference in the expression of miR-663 and miR-720 between zoledronate-treated group and a control group after 28 days of tooth extraction. The up-regulation of miR-663 was found in atherosclerotic plaque and the knockout of miR-663 resulting in promoting a repair of vascular endothelium via transforming growth factor beta 1 (TGF-β1) in a hyperuricemic rat model (Hong et al, 2015). Another finding demonstrated that the suppression of miR-720 and vasohibin1 (VASH1) resulted in stimulating of endothelial cell migration and vascular forming (Wang et al, 2014). Since an impairment of angiogenesis is one of the key mechanisms of MRONJ pathogenesis, the data from our study suggested the role of miR-34 in controlling an anti-angiogenic activity in MRONJ.

However, several limitations should be considered in this preliminary study. The number of study samples is limited due to the death of animals during study. Therefore, a statistical significance analysis could not be applied to strengthen the results. Furthermore, an immunohistochemical study should be performed in order to evaluate the function of osteoclast and also the number of blood vessels. In terms of miRNA analysis, there are still several miRNAs that might associate with the pathophysiological mechanism of MRONJ to be investigated; for example, miRNAs involved in promoting osteoclastic activity such as miR-21 and miR-31 or other miRNAs that have an influence on angiogenic activity, including miR-221, miR-126, miR-210 and miR-278. Altogether, future further investigation with a larger sample size will confirm the results from this study and provide an insightful information regarding the miRNA profile in bone tissue of MRONJ. An application of miRNA may warrant a future therapeutic approach for MRONJ patients.

5. Conclusion

In this study, the MRONJ was successfully developed in the SD rat model when treated with BPs. Six candidate miRNAs were found to be involving in the development of MRONJ. MiRNAs that affected an inhibition of osteoblast maturation, including miR-23a-3p, miR-23b-3p, miR27a-3p and miR-24-3p were upregulated in MRONJ bone tissue samples. Anti-angiogenesis-relating miRNAs such as miR-34-5p and miR-652-3p also moderately expressed in the MRONJ extraction sockets. This study suggested that the certain miRNAs have a role in controlling the cellular functions related to bone remodeling mechanisms and angiogenic activity in MRONJ. Still, a variety of miRNAs are of needed to be clarified their functions in which associated with pathophysiologic mechanisms of MRONJ.

6. Acknowledgements

The authors thank the Immunology Laboratory, Department of Periodontology and the Department of Microbiology, Faculty of Dentistry, Chulalongkorn University for providing laboratory facilities and technical support. We are also thankful to the Chulalongkorn University Laboratory Animal Center (CULAC) for experiment facilities and veterinary supports. This study was funded by Chulalongkorn University; Grant Number CU_GR_62_78_32-02.

7. References

Bartel, D. P. (2004). MicroRNAs: genomics, biogenesis, mechanism, and function. *cell, 116*(2), 281-297.

Black, D. M., Delmas, P. D., Eastell, R., Reid, I. R., Boonen, S., Cauley, J. A., . . . Man, Z. (2007). Once-yearly zoledronic acid for treatment of postmenopausal osteoporosis. *New England Journal of Medicine, 356*(18), 1809-1822.

Fish, J. E., Santoro, M. M., Morton, S. U., Yu, S., Yeh, R.-F., Wythe, J. D., . . . Srivastava, D. (2008). miR-126 regulates angiogenic signaling and vascular integrity. *Developmental cell, 15*(2), 272-284.

Ganda, K. (2013). *Dentist's Guide to Medical Conditions, Medications and Complications*: John Wiley & Sons.

Harris, T. A., Yamakuchi, M., Ferlito, M., Mendell, J. T., & Lowenstein, C. J. (2008). MicroRNA-126 regulates endothelial expression of vascular cell adhesion molecule 1. *Proceedings of the National Academy of Sciences, 105*(5), 1516-1521.

Hong, Q., Yu, S., Geng, X., Duan, L., Zheng, W., Fan, M., . . . Wu, D. (2015). High Concentrations of Uric Acid Inhibit Endothelial Cell Migration via miR-663 Which Regulates Phosphatase and Tensin Homolog by Targeting Transforming Growth Factor-β1. *Microcirculation, 22*(4), 306-314.

Howie, R. N., Borke, J. L., Kurago, Z., Daoudi, A., Cray, J., Zakhary, I. E., . . . Messer, R. (2015). A model for osteonecrosis of the jaw with zoledronate treatment following repeated major trauma. *PloS one, 10*(7).

Ito, T., Yagi, S., & Yamakuchi, M. (2010). MicroRNA-34a regulation of endothelial senescence. *Biochemical and biophysical research communications, 398*(4), 735-740.

Kaibuchi, N., Iwata, T., Yamato, M., Okano, T., & Ando, T. (2016). Multipotent mesenchymal stromal cell sheet therapy for bisphosphonate-related osteonecrosis of the jaw in a rat model. *Acta biomaterialia, 42*, 400-410.

Kühl, S., Walter, C., Acham, S., Pfeffer, R., & Lambrecht, J. T. (2012). Bisphosphonate-related osteonecrosis of the jaws–a review. *Oral oncology, 48*(10), 938-947.

Kuroshima, S., Sasaki, M., Nakajima, K., Tamaki, S., Hayano, H., & Sawase, T. (2018). Transplantation of Noncultured Stromal Vascular Fraction Cells of Adipose Tissue Ameliorates Osteonecrosis of the Jaw–Like Lesions in Mice. *Journal of Bone and Mineral Research, 33*(1), 154-166.

Lian, J. B., Stein, G. S., Van Wijnen, A. J., Stein, J. L., Hassan, M. Q., Gaur, T., & Zhang, Y. (2012). MicroRNA control of bone formation and homeostasis. *Nature Reviews Endocrinology, 8*(4), 212.

Liu, H., Dong, Y., Feng, X., Li, L., Jiao, Y., Bai, S., . . . Zhao, Y. (2019). miR-34a promotes bone regeneration in irradiated bone defects by enhancing osteoblastic differentiation of mesenchymal stromal cells in rats. *Stem cell research & therapy, 10*(1), 180.

Miksad, R. A., Lai, K.-C., Dodson, T. B., Woo, S.-B., Treister, N. S., Akinyemi, O., . . . Gazelle, G. S. (2011). Quality of life implications of bisphosphonate-associated osteonecrosis of the jaw. *The oncologist, 16*(1), 121-132.

Nissen, N. N., Polverini, P., Koch, A. E., Volin, M. V., Gamelli, R. L., & DiPietro, L. A. (1998). Vascular endothelial growth factor mediates angiogenic activity during the proliferative phase of wound healing. *The American journal of pathology, 152*(6), 1445.

Ruggiero, S., Dodson, T., & Fantasia, J. (2014). AAOMS position paper: Medication-related osteonecrosis of the jaw—2014 Update. *American Association of Oral and Maxillofacial Surgeons*.

Ruggiero, S. L., Dodson, T. B., Fantasia, J., Goodday, R., Aghaloo, T., Mehrotra, B., & O'Ryan, F. (2014). American Association of Oral and Maxillofacial Surgeons position paper on medication-related osteonecrosis of the jaw—2014 update. *Journal of Oral and Maxillofacial Surgery, 72*(10), 1938-1956.

Wang, H.-W., Huang, T.-S., Lo, H.-H., Huang, P.-H., Lin, C.-C., Chang, S.-J., . . . Tsai, C.-F. (2014). Deficiency of the microRNA-31–microRNA-720 pathway in the plasma and endothelial progenitor cells from patients with coronary artery disease. *Arteriosclerosis, thrombosis, and vascular biology, 34*(4), 857-869.

Wu, F., Yang, Z., & Li, G. (2009). Role of specific microRNAs for endothelial function and angiogenesis. *Biochemical and biophysical research communications, 386*(4), 549-553.

Yang, R., Tao, Y., Wang, C., Shuai, Y., & Jin, L. (2018). Circulating microRNA Panel as a Novel Biomarker to Diagnose Bisphosphonate-Related Osteonecrosis of the Jaw. *International journal of medical sciences, 15*(14), 1694.

Zandi, M., Dehghan, A., Malekzadeh, H., Janbaz, P., Ghadermazi, K., & Amini, P. (2016). Introducing a protocol to create bisphosphonate-related osteonecrosis of the jaw in rat animal model. *Journal of Cranio-Maxillofacial Surgery, 44*(3), 271-278.

Zhang, Y., Xie, R.-l., Croce, C. M., Stein, J. L., Lian, J. B., Van Wijnen, A. J., & Stein, G. S. (2011). A program of microRNAs controls osteogenic lineage progression by targeting transcription factor Runx2. *Proceedings of the National Academy of Sciences, 108*(24), 9863-9868.